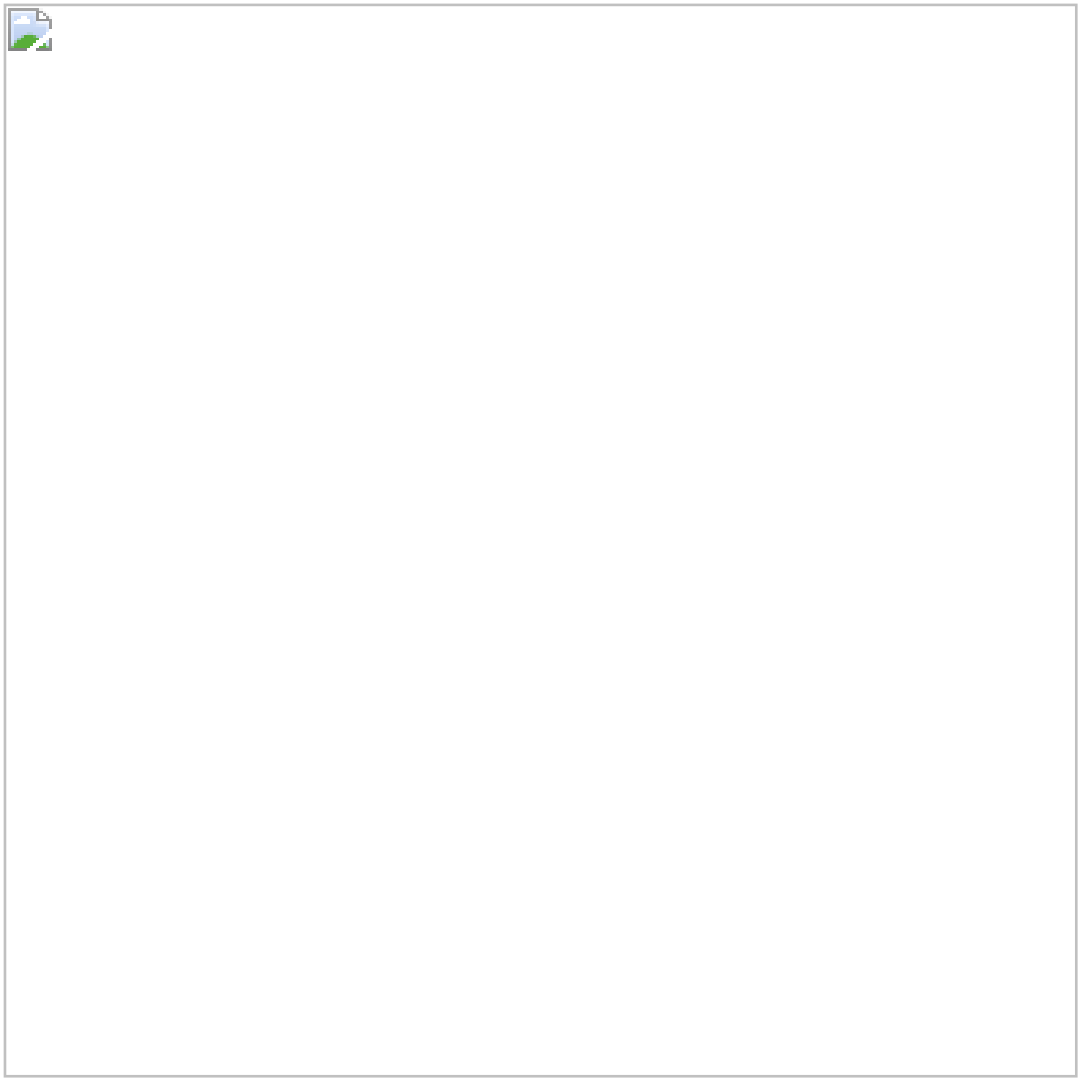

Generation of a Transcriptional Radiation Exposure Signature in Human Blood Using Long-Read Nanopore Sequencing

Authors: Cruz-Garcia, Lourdes, O'Brien, Grainne, Sipos, Botond, Mayes, Simon, Love, Michael I., et al.

Source: Radiation Research, 193(2) : 143-154

Published By: Radiation Research Society

URL: https://doi.org/10.1667/RR15476.1

RADIATION RESEARCH **193**, 143–154 (2020)
0033-7587/20 $15.00

DOI: 10.1667/RR15476.1

Generation of a Transcriptional Radiation Exposure Signature in Human Blood Using Long-Read Nanopore Sequencing

Lourdes Cruz-Garcia,[a] Grainne O'Brien,[a] Botond Sipos,[b] Simon Mayes,[b] Michael I. Love,[c,d] Daniel J. Turner[b] and Christophe Badie[a,1]

[a] *Cancer Mechanisms and Biomarkers Group, Radiation Effects Department, Centre for Radiation, Chemical and Environmental Hazards Public Health England Chilton, Didcot, OX11 ORQ United Kingdom;* [b] *Oxford Nanopore Technologies, OX4 4DQ, Oxford, United Kingdom; and Departments of* [c] *Biostatistics and* [d] *Genetics, University of North Carolina at Chapel Hill, Chapel Hill, North Carolina, 27516*

Cruz-Garcia, L., O'Brien, G., Sipos, B., Mayes, S., Love, M.I., Turner, D.J. and Badie, C. Generation of a Transcriptional Radiation Exposure Signature in Human Blood Using Long-read Nanopore Sequencing. *Radiat. Res.* 193, 143–154 (2020).

In the event of a large-scale event leading to acute ionizing radiation exposure, high-throughput methods would be required to assess individual dose estimates for triage purposes. Blood-based gene expression is a broad source of biomarkers of radiation exposure which have great potential for providing rapid dose estimates for a large population. Time is a crucial component in radiological emergencies and the shipment of blood samples to relevant laboratories presents a concern. In this study, we performed nanopore sequencing analysis to determine if the technology can be used to detect radiation-inducible genes in human peripheral blood mononuclear cells (PBMCs). The technology offers not only long-read sequencing but also a portable device which can overcome issues involving sample shipment, and provide faster results. For this goal, blood from nine healthy volunteers was 2 Gy *ex vivo* X irradiated. After PBMC isolation, irradiated samples were incubated along with the controls for 24 h at 37°C. RNA was extracted, poly(A)+ enriched and reverse-transcribed before sequencing. The data generated was analyzed using a Snakemake pipeline modified to handle paired samples. The sequencing analysis identified a radiation signature consisting of 46 differentially expressed genes (DEGs) which included 41 protein-coding genes, a long non-coding RNA and four pseudogenes, five of which have been identified as radiation-responsive transcripts for the first time. The genes in which transcriptional expression is most significantly modified after radiation exposure were APOBEC3H and FDXR, presenting a 25- and 28-fold change on average, respectively. These levels of transcriptional response were comparable to results we obtained by quantitative polymerase chain reaction (qPCR) analysis. *In vivo* exposure analyses showed a transcriptional radioresponse at 24 h postirradiation for both genes together with a strong dose-dependent response in blood irradiated *ex vivo*. Finally, extrapolating from the data we obtained, the minimum sequencing time required to detect an irradiated sample using APOBEC3H transcripts would be less than 3 min for a total of 50,000 reads. Future improvements, in sample processing and bioinformatic pipeline for specific radiation-responsive transcript identification, will allow the provision of a portable, rapid, real-time biodosimetry platform based on this new sequencing technology. In summary, our data show that nanopore sequencing can identify radiation-responsive genes and can also be used for identification of new transcripts.

INTRODUCTION

Over the last decade, gene expression analysis has emerged as a realistic approach for assessing radiation exposure in human blood samples after medical exposure or during emergency situations, due to its high throughput and time efficiency (*1–4*). Although many studies have used microarrays (*5, 6*), qPCR analyses have proven to provide accurate dose estimates by focusing on specific radiation-responsive genes (*7–15*) in only 7 h (*16*) and now in only 4 h (*17*). This methodology has been validated through several NATO and RENEB exercises (*16, 18, 19*). A single gene expression analysis [e.g., ferredoxin reductase, (FDXR), also reported to be a protein biomarker of radiation exposure, (*20*)] can offer accurate information on dose received *in vivo* in humans across a large range of doses from CT scan to total-body exposure (*14*). However, a radiation signature can provide further information about homogeneity of exposure (*21*), mixed exposure (*22*) or dose rate (*11*). The transcriptomic profiles can provide distinctive gene expression patterns useful for later reconstruction of exposure characteristics. Transcriptomic analyses by microarrays (*11, 23*) and next-generation sequencing techniques either targeted (*24*) or specifically for microRNA tran-

Editor's note. The online version of this article (DOI: https://doi.org/10.1667/RR15476.1.S1) contains supplementary information that is available to all authorized users.

[1] Address for correspondence: Radiation Effects Department, Centre for Radiation, Chemical and Environmental Hazards Public Health England Chilton, Didcot, Oxfordshire OX11 ORQ, UK; email: christophe.badie@phe.gov.uk.

scriptome (*25*) can identify a radiation-response signature. However, some of these techniques have limitations; they can be time consuming, relying on existing knowledge of transcriptome sequences and requiring advanced bioinformatic tools and expertise (*26, 27*). On the other hand, the so-called third-generation sequencing methods, either single-molecule real-time sequencing developed by Pacific Biosciences (Menlo Park, CA) (*28*) or nanopore sequencing offered by Oxford Nanopore Technologies (Oxford, UK) (*29–31*), provide full-length transcripts unlike the second-generation sequencing techniques. The approach of Pacific Bioscience is based on sequencing by synthesis reactions occurring in zero-mode waveguides, which provide real-time sequencing for thousands of reactions simultaneously (*32*). Nanopore sequencing consists of passing DNA/RNA molecules through a biological pore driven under an electric field and recording changes in the ionic current as nucleobases pass through the pore. For biodosimetry, nanopore sequencing offers the advantages of high-throughput, low-cost, real-time sequencing and the possibility of using a portable device. This portable device from Oxford Nanopore Technologies, referred to as MinION, is a small, light-weight (under 100 g) sequencer, which can be powered to a laptop in which data are transferred through a USB connection during real-time sequencing. This device has already been used and reported to operate efficiently outside the laboratory for DNA sequencing in numerous environments, including the rain forest (*33*), the Antarctic (*34*) and on the International Space Station (*35*). Therefore, it is clearly plausible that this sequencing technology could be developed and used ''in the field'' for transcriptomic analyses in the event of a major radiological or nuclear emergency, bypassing the need to ship blood samples to a specialized laboratory; consequently, this feature will considerably shorten the time required to provide dose estimations.

In the current study, we developed a protocol and a bioinformatic pipeline to demonstrate the suitability of the nanopore technology to generate a radiation-induced transcriptomic signature in human peripheral blood mononuclear cells (PBMCs). Moreover, we demonstrated its usefulness to discover new radiation biomarkers. The future development of a biodosimetry platform based on nanopore technology is also presented.

MATERIALS AND METHODS

Blood Irradiation Ex Vivo

Blood from nine healthy donors (Supplementary Table S1; https://doi.org/10.1667/RR15476.1.S1) was collected and received either 0 or 2 Gy X-rays at a dose rate of 0.5 Gy min^{-1} (10 ml of blood per condition per donor) (Fig. 1). Irradiations were performed at room temperature using an A.G.O. HS X-ray system (Aldermaston, Reading, UK; output 13 mA, 250 kV peak, 0.5 Gy/min). The dose of 2 Gy was chosen due to its wide use as the therapeutic dose delivered during radiation treatments and because this dose surpasses the threshold for acute radiation syndrome (1 Gy). After irradiation, the PBMCs were isolated using Histopaque®-1077 (Sigma-Aldrich, Poole, UK) and maintained in LGM-3 culture media (Lonza, Slough, UK) at 2×10^6 cells ml^{-1} for 24 h at 37°C in a humidified 5% CO_2 atmosphere. After 24 h, the PBMCs were pooled in groups of three donors each (PBMCs pooled from 30 ml of blood originally) and stored at –80°C until RNA extraction. Venous blood was taken at the Centre for Radiation, Chemical and Environmental Hazards, Public Health England (Chilton, UK) with informed consent and the ethical approval of the West Midlands - Solihull Research Ethics Committee (no. REC 14/WM/1182).

Dose-Response Experiment

Blood from seven healthy donors (Supplementary Table S1; https://doi.org/10.1667/RR15476.1.S1) was collected and exposed to a range of X ray doses (0.25, 0.5, 1 and 2 Gy at a dose rate of 0.5 Gy min^{-1}). After 24 h, RNA was extracted using a RiboPure™-Blood RNA Purification Kit (Thermo Fisher Scientific, Loughborough, UK). The cDNA was synthesized from 350 ng of RNA using High Capacity cDNA Reverse Transcription Kit (Applied Biosystems®, Foster City, CA).

Radiotherapy Patient Samples

Blood samples from a previous study (*13, 36*) were analyzed to monitor the radiation response *in vivo* of apolipoprotein B mRNA editing enzyme catalytic subunit 3H (APOBEC3H) and FDXR. This cohort was comprised of patients with the following cancer diagnoses (n): endometrial (4), breast (5), lung (4), prostate (3), esophageal (2) and colon (1). Patients received intensity modulated radiotherapy using a linear accelerator. Blood samples were collected at three different time points during the course of the treatment: before the start of the treatment, 0.5–2 h and 24 h after receiving the first fraction. The prescribed doses for each patient are described elsewhere (*13, 36*).

Sequencing Analysis

The full-length sequencing by Oxford Nanopore Technologies was performed using a PromethION sequencer (Oxford Nanopore Technologies) with the libraries prepared using the PCS109 kit according to the instructions (https://bit.ly/2Qx8z7o).

RNA was extracted using the RNeasy Midi Kit (QIAGEN, Manchester, UK). The quantity of isolated RNA was determined by spectrophotometry using an ND-1000 NanoDrop (Thermo Fisher Scientific™ Inc., Waltham, MA) and quality was assessed using a TapeStation 2200 (Agilent Technologies Inc., Santa Clara, CA). Before the library was prepared, the RNA was poly(A)+ enriched using an Oligotex mRNA Mini Kit (QIAGEN) and the cDNA was prepared from 1 ng of RNA using strand-switching and VN primers. After the cDNA synthesis, a selective PCR amplification was performed for full-length transcripts before specific adapters were added to start the sequencing run in the PromethION sequencer. The samples were run in two SpotON flow cells per sample in a PromethION sequencer.

To compare the sequencing versus qPCR analyses, cDNA was prepared from 50 ng of the poly(A)+-enriched RNA using the High-Capacity cDNA Reverse Transcription Kit (Applied Biosystems) according to the manufacturer's protocol. The cDNA was used for the qPCR analyses as described in its respective section below.

Quantitative Real-Time Polymerase Chain Reaction

qRT-PCR was performed using a Rotor-Gene Q (QIAGEN, Hilden, Germany) with PerfeCTa MultiPlex qPCR SuperMix (Quanta Biosciences Inc., Gaithersburg, MD). The samples were run in triplicate in 10 μl reactions with 1 μl of the cDNA synthesis reaction, containing 1 ng poly (A)+ (validation sequencing analysis) or 7 ng of total RNA (dose-response and *in vivo* analyses) converted to cDNA,

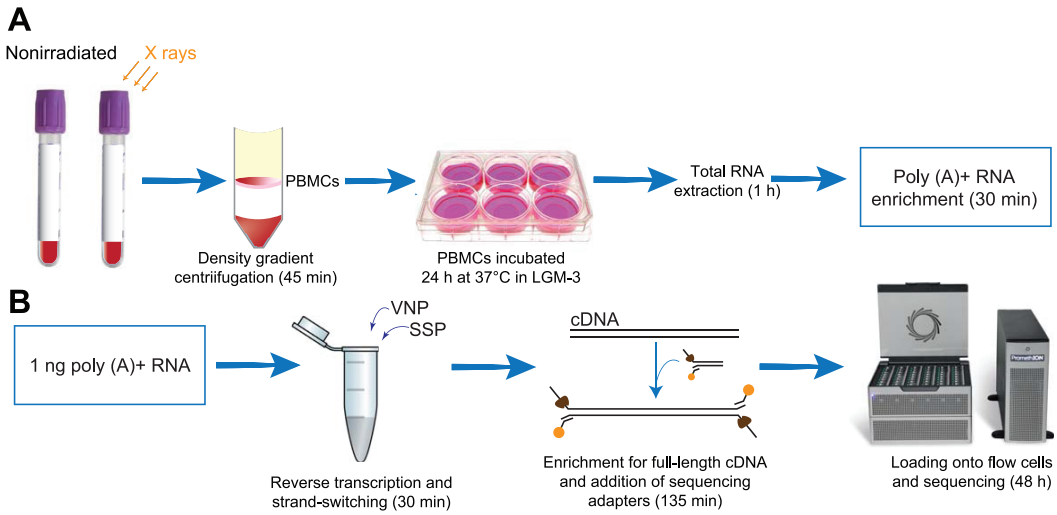

FIG. 1. Experimental workflow. Panel A: Blood from nine healthy donors (20 ml per donor), which was sham or 2 Gy irradiated (dose rate 0.5 Gy min^{-1}) *ex vivo*, was used to isolate PBMCs by a density gradient centrifugation. The PBMCs were incubated for 24 h at 37°C before the RNA was extracted. The total RNA obtained was poly(A)+ enriched to remove ribosomal RNAs from the samples. Panel B: A total of 1 ng from the poly(A)+-enriched RNA was used for the sequencing analysis. The RNA was reverse transcribed using VN and strand-switching (SSP) primers. A PCR amplification step was performed to enrich the samples for full-length cDNAs followed by the addition of sequencing adapters. The samples were run in two SpotON flow cells per sample in a PromethION sequencer. The time required for each step of the protocol is included in the diagram.

together with five different sets of primers and fluorescent probes at 300 n*M* concentration each. 3′6-Carboxyfluorescein (FAM), 6-hexachlorofluorescein (HEX), Atto 680, Atto 390 and Texas Red (Eurogentec Ltd., Fawley, Hampshire, UK) were used as fluorochrome reporters for the probes analyzed in multiplexed reactions with five genes per run including a housekeeping gene. Primer sequences for FDXR, APOBEC3H, GADD45A and DDB2 are listed in Supplementary Table S2; https://doi.org/10.1667/RR15476.1.S1. The reactions were performed with the following cycling conditions: 2 min at 95°C, then 45 cycles of 10 s at 95°C and 60 s at 60°C. Data were collected and analyzed by Rotor-Gene Q Series software. Gene target cycle threshold (Ct) values were normalized to hypoxanthine phosphoribosyltransferase 1 (HPRT1) internal control. Cycle threshold values were converted to transcript quantity using standard curves obtained by serial dilution of PCR-amplified DNA fragments of each gene. The linear dynamic range of the standard curves covering six orders of magnitude (serial dilution from 3.2×10^{-4} to 8.2×10^{-10}) gave PCR efficiencies between 90 and 103% for each gene with $R^2 > 0.998$.

Data Analysis

Nanopore cDNA reads were analyzed using a Snakemake pipeline modified to handle paired samples (*37*). The pipeline (https://bit.ly/3403pVc) maps the reads to the transcriptome using minimap2 (*38*) and estimates per-transcript read counts using salmon (*39*). After the aggregation of transcript counts into gene counts based on the Ensembl annotation, differential gene expression was detected using the quasi-likelihood method provided by the edgeR (*40*) Bioconductor package.

Statistical Analysis

Statistical analyses were performed using Minitab software (State College, PA). Data are presented as means ± standard deviation (SD) or standard error of the mean (SEM). Comparisons were analyzed using Student's *t* test. A significance of $P \leq 0.05$ was applied to all statistical tests performed. Pearson's correlation analyses were performed to verify dose-response relationships and for comparison purposes between sequencing and qPCR analyses. To measure the consistency of the gene expression response to radiation, the coefficient of variation (CV, mean-normalized standard deviation) was calculated for all the differentially expressed genes (DEGs).

RESULTS

Nanopore Long-reads Sequencing

Three biological replicate experiments, each including isolated PBMCs from three different donors pooled together, were performed. Multiple blood samples were pooled together so that enough poly (A)+-enriched RNA could be isolated for the sequencing analysis, since the maximum amount of blood we were permitted to obtain per donor was 20 ml. After total RNA extraction from PBMCs, the samples were enriched in poly(A)+ RNA to discard ribosomal RNA from the sequencing analyses. The RNA integrity number (RIN) values obtained for the different RNA extractions ranged from 8.8 to 9.2, demonstrating good-quality RNAs. The RNA extraction and poly(A)+ enrichment from the blood samples required 90 min and the library preparation 165 min. The flow cells were run for 48 h in a PromethION and the data analysis required a day.

The samples were run for 48 h to generate library sizes of 40–75 million primary aligned reads (Fig. 2A) and a total of 25,656 mRNAs and 110,829 transcript variants were identified. These read differences between samples could be associated with inconsistencies between flow cells or small differences in adapter ligation efficiency between libraries.

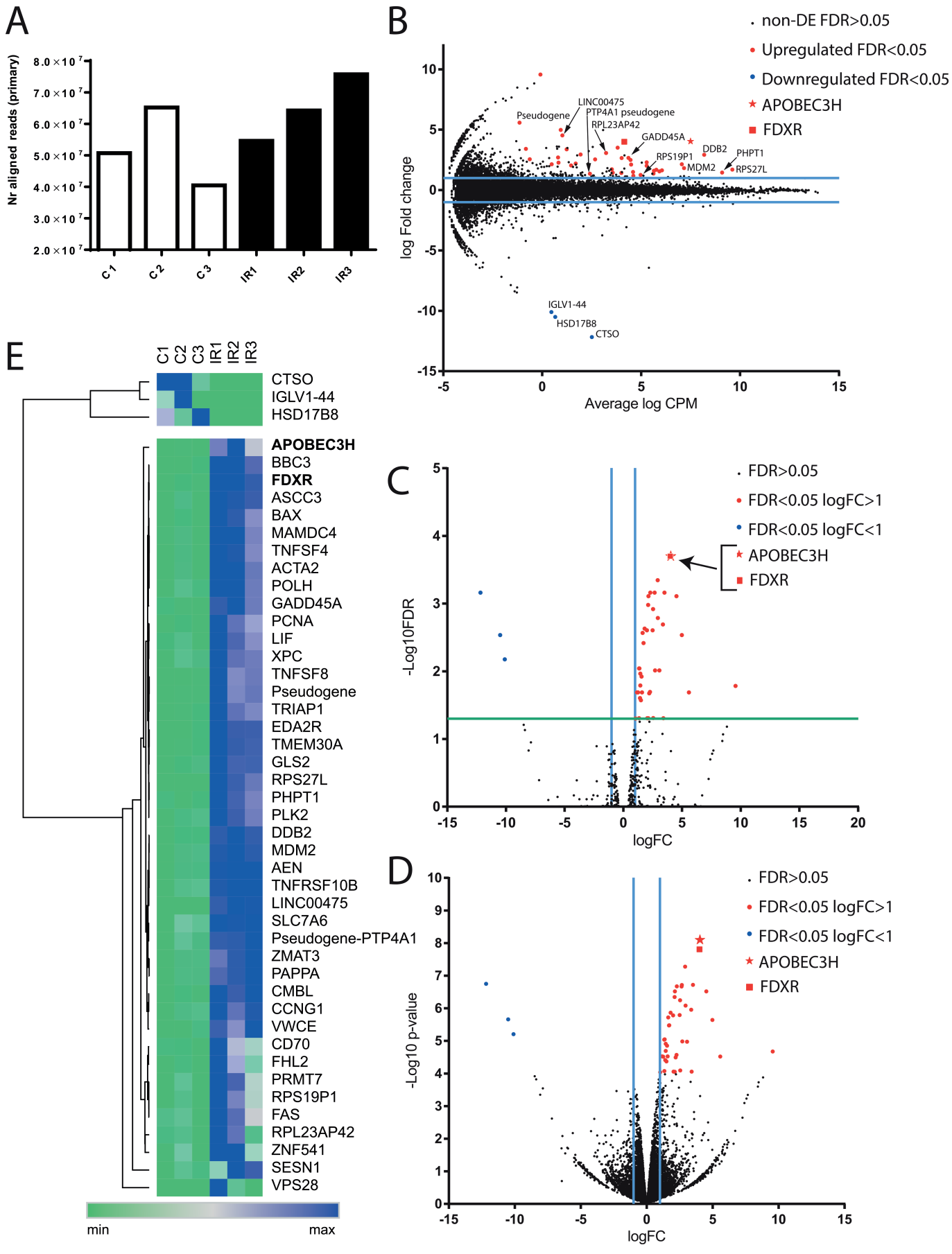

Differential Gene Expression Analysis

In our protocol, PBMCs were analyzed 24 h postirradiation; at this time point, 41 protein-coding genes, 1 long non-coding RNA and 4 pseudogenes were identified as significantly ($P < 0.00009$) differentially expressed (Fig. 2B–E, Supplementary Table S3; https://doi.org/10.1667/RR15476.1.S1) with false discovery rates (FDR) ranging from 0.0002 for the most significant DEGs after irradiation, FDXR and APOBEC3H, to 0.049 for Fas cell surface death receptor (FAS). When the control was compared to the irradiated samples (Fig. 2B), the majority of the DEGs were upregulated, with only cathepsin O (CTSO), hydroxysteroid 17-beta dehydrogenase 8 (HSD17B8) and immunoglobulin lambda variable 1-44 (IGLV1-44) being significantly downregulated.

The number of read counts for APOBEC3H was higher than FDXR (Figs. 2B and 3A), with background counts going from 957 ± 181 between the three sequencing repeats and 98 ± 21 to 16,423 ± 520 and 1,587 ± 84 (counts per 50×10^6 aligned reads), respectively, demonstrating a higher endogenous level of transcription. On average, after irradiation, the DEGs presenting higher counts were ribosomal protein S27 like (RPS27L) followed by phosphohistidine phosphatase 1 (PHPT1) (Fig. 2B). The volcano plots shown in Fig. 2 allow for visualization of the samples regarding the FDR (Fig. 2C) and *P* value (Fig. 2D) compared to the fold change (FC) showing the most significant genes, APOBEC3H and FDXR, highlighted at the top of the graph.

The long non-coding RNA identified was the long intergenic non-protein coding RNA 475 (LINC00475) presenting a consistent 30 ± 2.2-fold increase in irradiated samples.

Moreover, to the best of our knowledge, CTSO, IGLV1-44, protein tyrosine phosphatase type IVA, member 1 (PTP4A1) pseudogene (ENSG00000278275), a novel pseudogene (ENSG00000283234), ribosomal protein L23a pseudogene 42 (RPL23AP42) and ribosomal protein S19 pseudogene 1 (RPS19P1) have been identified as radiation-responsive transcripts for the first time. Interestingly, two genes were significantly downregulated, CTSO counts ranged from 184–739 per 50×10^6 primary aligned reads in the control sample, while no counts were detected in the irradiated samples (Supplementary Table S3; https://doi.org/10.1667/RR15476.1.S1). For IGLV1-44, 120 and 253 counts were detected in two control samples and no counts were detected on the remaining samples. RPL23AP42 and RPS19P1were upregulated to 14 ± 8- and 3.4 ± 0.96-fold change, respectively. The novel pseudogene showed a high-fold change of 54 ± 12.1 but was present at lower counts compared to the majority of DEGs (Fig. 2B).

Hierarchical clustering of DEGs (Fig. 2C), using the Morpheus software package (https://software.broadinstitute.org/morpheus/), showed separate clusters for the up- and downregulated genes. From the 46 DEGs, most of the genes (35 genes) showed a very consistent response to radiation between replicates, with coefficients of variation between 0 and 20.2% (Supplementary Table S3; https://doi.org/10.1667/RR15476.1.S1), while a few were less consistently upregulated between experiments, in particular, FHL2, RPL23AP42 and VPS28.

Comparison of RNA Sequencing and qPCR Analysis

The number of read counts for APOBEC3H, FDXR and GADD45 genes were consistent among the three experiments (Fig. 3A). The level of expression was approximately 10 times higher for APOBEC3H compared to FDXR, while fold changes were very similar (Fig. 3A). Four genes were selected to compare their response to radiation using sequencing and qPCR analyses. The sequencing gene transcript counts were normalized to HPRT1 transcript copies and compared to qPCR analysis data obtained in parallel (also normalized to HPRT1 transcript copies) (Fig. 3B). The three most significantly expressed genes were selected (APOBEC3H, FDXR and DDB2) together with GADD45 due to its known response to radiation and the fact that no transcript variants were detected for this gene, simplifying the design for PCR primers. Importantly, the results showed similar response between control and irradiated samples by sequencing and qPCR for APOBEC3H, FDXR and GADD45 (Fig. 3B, Supplementary Table S4; https://doi.org/10.1667/RR15476.1.S1). Linear regression analysis of the correlation between qPCR and sequencing data showed a strong correlation between both techniques for APOBEC3H, FDXR and GADD45, with R^2 of 0.9837 and Pearson's correlation coefficient of 0.992 (Supplementary Fig. S1).

However, the radiation response of DDB2 was significantly lower by qPCR than sequencing (Fig. 4) (13.3 vs. 7.4 fold). This discrepancy was unexpected, since the results were comparable for the other three genes examined; we therefore sought to determine an explanation. We identified

←

FIG. 2. Gene expression analysis of *ex vivo* irradiated blood by long-read nanopore RNA sequencing. Panel A: Sequencing depth per library (number of reads per sample/library). Panel B: MA plot showing the differential expressed genes between the control and irradiated samples. The blue lines indicate genes that are up- or downregulated two-fold. Panel C: Volcano plot representing the FDR (–log10 FDR) versus fold change (log FC). The green line indicates a FDR value of 0.05. Panel D: Volcano plot representing significance (–log10 *P* value) versus fold change (log FC). Panel E: Heatmap of the normalized counts to HPRT. The 46 genes significantly regulated by radiation exposure were grouped by hierarchical clustering. Differential gene expression was detected using the quasi-likelihood method provided by the edgeR.

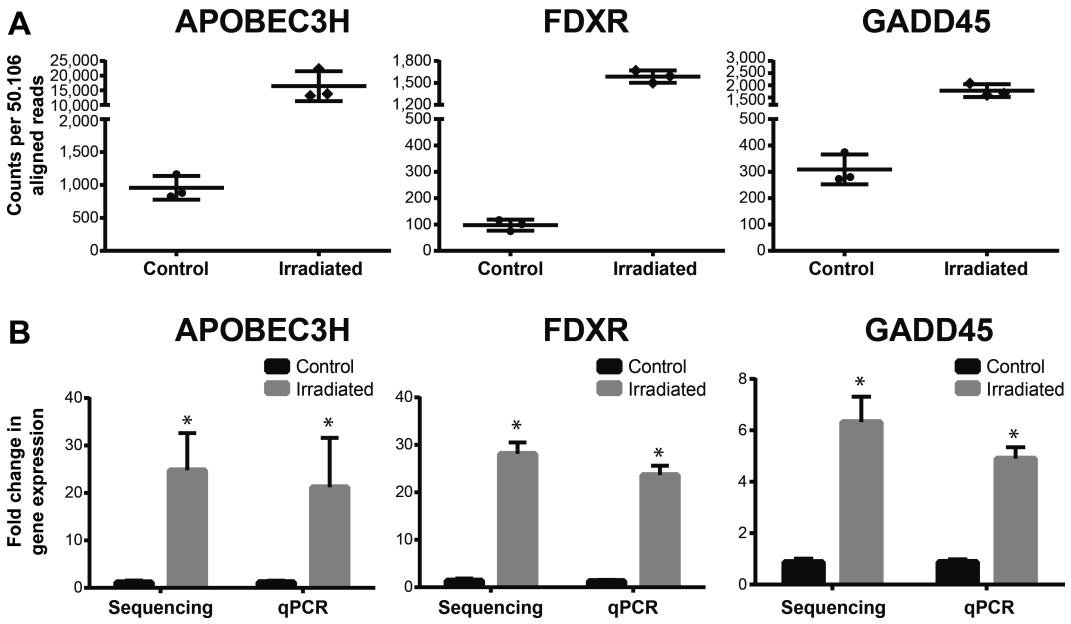

FIG. 3. Number of read counts per gene and comparison of the radiation response of APOBEC3H, FDXR and GADD45 by nanopore long-read sequencing analysis versus qPCR. Panel A: The abundance of reads per gene is shown for the control and irradiated samples (counts normalized by library size). Panel B: The fold change between the control and irradiated samples was compared between sequencing and qPCR analyses. Data are shown as mean ± standard deviation. No significant differences were observed (*t* test, $P < 0.05$) between sequencing and qPCR analysis. *Significant differences between control and irradiated sample (*t* test, $P \leq 0.05$).

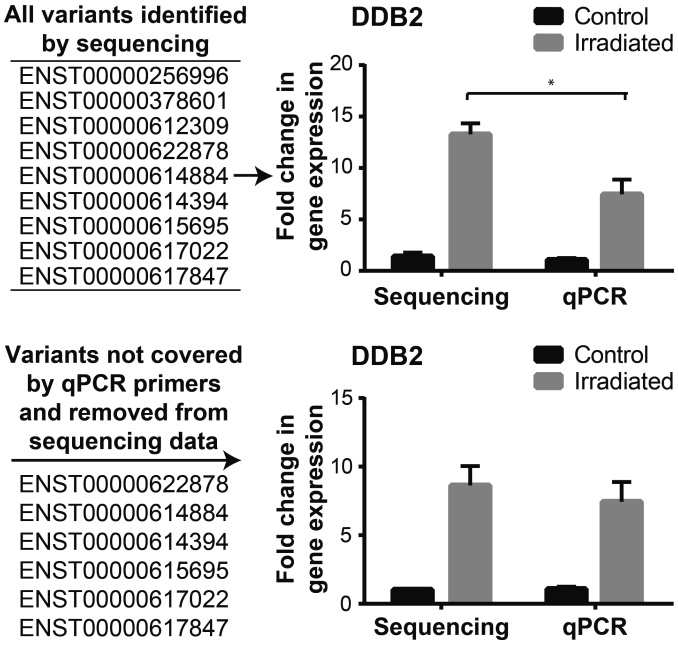

FIG. 4. Effect of transcript variant identification by nanopore sequencing on radiation response. The fold change for DDB2 was compared between nanopore sequencing and qPCR analyses, including or excluding specific transcript variants. The variants excluded were not detected with the qPCR primer designs. *Statistically significant differences (*t* test, $P \leq 0.05$).

nine transcript variants by sequencing for DDB2. Some were not covered using the qPCR primers we designed, and therefore were not detected and quantified, which could be the source of the difference. To confirm our hypothesis, those transcript variant data were removed from the sequencing data, which as we hypothesize, led to similar DDB2 fold of change between techniques. Thus, in the case of DDB2, sequencing data provided a more complete picture of the radiation-induced expression profile, as some transcript variants were missed using our qPCR analyses.

Gene Expression Dose Response of APOBEC3H and FDXR in Whole Blood Irradiated Ex Vivo

To confirm APOBEC3H as a valid radiation-responsive gene usable for biological dosimetry purposes, we generated a dose response for both the APOBEC3H and FDXR genes in whole blood X-ray irradiated *ex vivo* using six doses ranging from 0.25 to 4 Gy (Fig. 5). Indeed, both genes showed a strong dose-dependent response to radiation with similar profiles; FDXR showed slightly higher fold changes at all doses (Fig. 5). Inter-individual variability among the seven donors did not demonstrate a clear difference between both genes. Dose-response curves for each gene are shown with their respective linear fits (Supplementary Fig. S2; https://doi.org/10.1667/RR15476.1.S1), with linear R^2 values of 0.931 and Pearson's correlation coefficient of 0.965 for APOBEC3H and 0.9126 and 0.955 for FDXR. A strong positive linear relationship between dose and gene expression was observed in males for FDXR and APOBEC3H

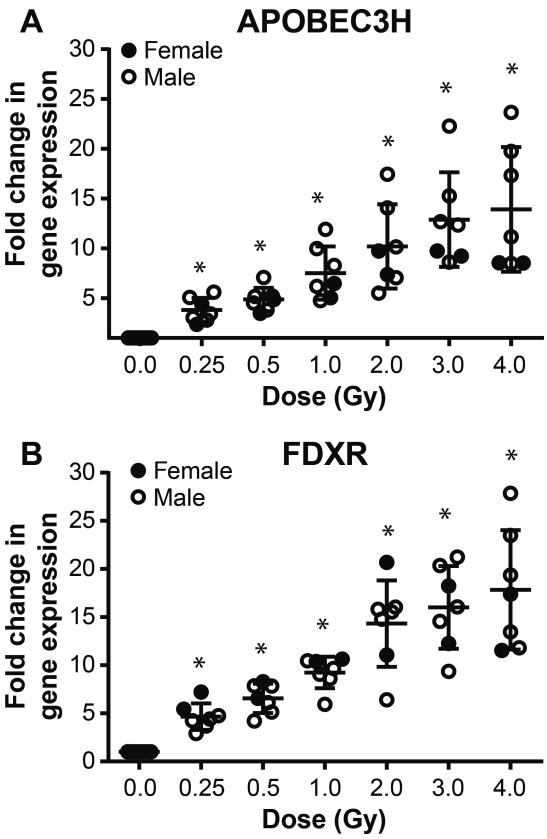

FIG. 5. Dose-response analyses of APOBEC3H and FDXR. Multiplexed QRT-PCR gene expression fold changes of APOBEC3H and FDXR (panels A and B, respectively) 24 h postirradiation in blood samples from seven healthy donors exposed *ex vivo* to a range of doses (0.25, 0.5, 1, 2, 3, 4 Gy; 0.5 Gy min^{-1}). *Significantly different from control (paired *t* test, $P \leq 0.001$).

(Supplementary Fig. S3 and S4). Although the correlation between dose and gene expression was significant for females, their Pearson's coefficient and R^2 value were lower than for males (Supplementary Fig. S3 and S4); however, it should be noted that only two female samples were available for this experiment.

Gene Expression Profile of APOBEC3H and FDXR in In Vivo Irradiated Blood Samples from Cancer Patients During Radiotherapy

Since APOBEC3H was not a gene we identified in previous experiments, we next sought to confirm the validity of APOBEC3H transcriptional expression compared to FDXR for which we validated responsiveness *in vivo* in human blood samples. Both genes were monitored in six different types of cancer patients who received radiotherapy, at 2 h and 24 h after the first fraction, for a total of 19 patients (Fig. 6). Interestingly, the results showed an upregulation of APOBEC3H as early as 2 h after the first radiotherapy fraction and confirmed the upregulation at the 24-h postirradiation time point with a 1.9-fold change. FDXR was upregulated after 24 h, presenting a slightly

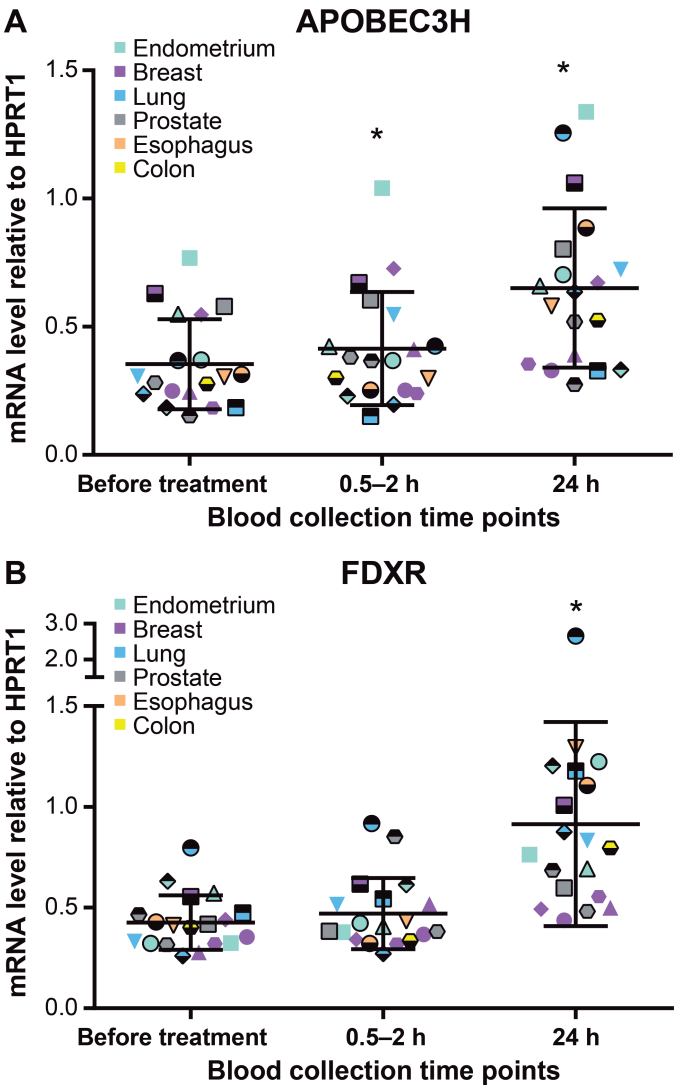

FIG. 6. mRNA expression levels of APOBEC3H and FDXR (panels A and B, respectively) in blood from radiotherapy patients. Blood samples from 19 patients, comprising those with endometrial, breast, lung, prostate, esophageal and colon cancer, were analyzed. Blood was collected at three time points: before the start of the treatment, at 0.5–2 h and 24 h after the first fraction. Individual data points are shown for all patients, together with the mean ± SD (each patient is represented with a different symbol). Each cancer group was color coded. Statistical analyses were performed in log-transformed data. *Significantly different from the control (before treatment) (paired *t* test, $P \leq 0.05$).

higher upregulation than APOBEC3H with a 2.2-fold change.

Kyoto Encyclopedia of Genes and Genomes (KEGG) Pathway Analysis

To assess the pathways in which the genes identified by these long-read sequencing experiments were involved, KEGG pathway analysis was performed (http://www.genome.jp/kegg/). The DEGs were assigned to 95 KEGG pathways. The top 10 enriched pathways are shown in Fig. 7. As anticipated for this dose level in blood, the p53

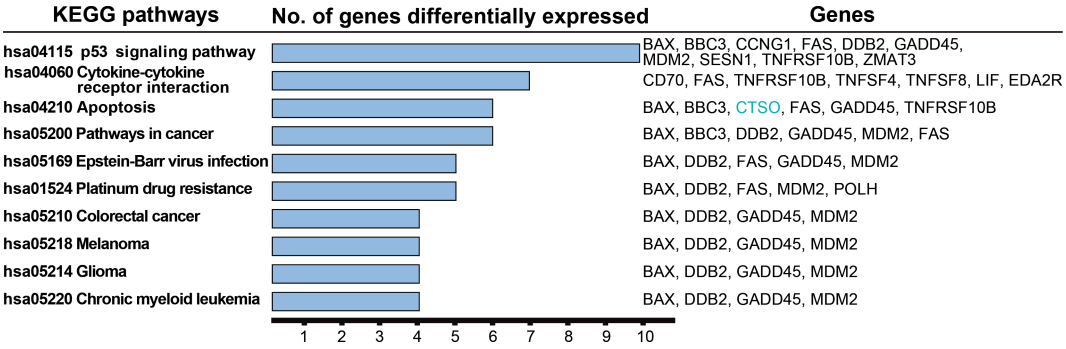

FIG. 7. KEGG pathway analysis for DEGs between control and irradiated PBMCs. All the genes listed were upregulated apart from CTSO (highlighted in blue).

signaling pathway was the most represented by the DEGs, followed by cytokine-cytokine receptor interaction and apoptosis.

DISCUSSION

To our knowledge, this is the first study in which ''third generation sequencing'' nanopore technology has been employed to provide a radiation-induced gene expression signature useable for biological dosimetry purposes. Nanopore sequencing analysis of human PBMCs irradiated *ex vivo* has identified over 25,000 different transcripts with 46 genes showing a radiation-dependent significant shift in expression; in particular, two of these genes, APOBEC3H and FDXR, were clearly the most significantly responsive genes to ionizing radiation, with fold changes between 25 to 28 fold in average for the dose delivered (2 Gy). Identifying FDXR was reassuring, and validated the long-read sequencing technology, as it has been previously characterized *ex vivo* by other methods (*8, 10, 15, 16, 23*) and validated in human *in vivo*, demonstrating its suitability to provide accurate dose estimation in *in vivo* partial- or total-body irradiated individuals (*14*). However, although APOBEC3H has been previously mentioned as a radiation-responsive gene (*41*), it had not been very well characterized. The APOBEC family of enzymes is comprised of single-stranded DNA cytosine deaminases which restrict replication of DNA-based parasites (*42*). Although the role of APOBEC3H in the radiation-induced DNA damage response is unknown as far as we know, its response to radiation is probably ATM-BRCA1-dependent (*43*).

In this study, perhaps surprisingly, the gene APOBEC3H showed a very strong response to radiation in isolated PBMCs, similar to FDXR, the most strongly upregulated gene identified in human blood in multiple studies from our laboratory; it was slightly lower in whole blood compared to FDXR. While small, these differences could be attributed to the expression level in cell subpopulations present in whole blood compared to isolated PBMCs. APOBEC3H transcriptional response to radiation in *ex vivo* irradiated blood followed a sublinear dose-response relationship similar to FDXR. Dose estimates provided with FDXR have proven to be very accurate at low and high doses (*14*) and have been used successfully in exercises on blind samples (*16, 18, 19*). The similar dose-response curve observed for APOBEC3H suggests that this gene could become a useful, possibly standalone biomarker of radiation exposure for dose estimations in humans.

We have presented the first expression profile of APOBEC3H in radiotherapy patient blood samples obtained before and after the first treatment fraction, to determine if its expression can indeed be detected *in vivo* in partial-body irradiated samples. Importantly, APOBEC3H was upregulated after 24 h as FDXR, but also interestingly, at a much earlier time point in the range of 0.5–2 h after the first fraction of radiotherapy. To note, FDXR did not show a significant upregulation at such earlier time postirradiation, making APOBEC3H an informative biomarker even in cases of blood sampling early after irradiation. Although both genes showed a strong dose-response correlation, APOBEC3H showed higher variability in its radiation response, as observed in its coefficient of variability.

The question of sex-dependent radiation response of APOBEC3H has been previously raised (*41*), but different results were observed with different technical approaches (microarray and qPCR analyses). In the current study, male and female dose-response correlation analysis for APOBEC3H presented significant correlations, but female linear fit had a slightly lower R^2 value, indicating higher variability of responses. The female group was represented by two individuals; therefore, there were not enough subjects in each sex group to demonstrate a sex-dependent effect on APOBEC3H response to radiation. Although further investigations are required, the strong radiation response of APOBEC3H makes it a biomarker of exposure in blood *ex vivo* and *in vivo*, identified by long-read sequencing and confirmed by qPCR.

The majority of genes included in the radiation-induced gene signature identified by nanopore technology have been previously described as radiation-responsive genes in multiple studies (e.g., *8, 23, 44–46*). However, to the best of our knowledge, and after screening of the literature, CTSO, IGLV1-44 and four pseudogenes [PTP4A1-pseudo-

gene, a novel pseudogene (ENSG00000283234), RPL23AP42 and RPS19P] had not been previously reported and were identified perhaps for the first time as radiation-responsive in this study using nanopore long-read sequencing. Pseudogenes are genomic sequences resembling protein-coding genes which result from inactivating gene mutations during evolution. Pseudogenes lack coding potential, present tissue-specific and constitutive expression profiles (*47*) and have regulatory effects on protein-coding gene expression (*48, 49*). Pseudogenes have been reported as survival prognosis markers in some cancers (*50, 51*) and to be responsive to ionizing radiation (*52, 53*), although to date, their potential as biomarkers of radiation exposure has not been addressed. RPL23AP42 and RPS19P are ribosomal associated pseudogenes, which indicate that radiation modulates translation processes in the cells, as suggested elsewhere (*52*). Therefore, nanopore sequencing has demonstrated its potential as a biodosimetry tool and for the discovery of new biomarkers of radiation exposure.

Nanopore sequencing provides long-reads, thus eliminating the ambiguities associated with splice variant and isoform calling. The sequencing data presented for each DEG includes all the variants identified for each gene. When the sequencing data were compared with the qPCR analysis (Figs. 3 and 4), differences in radiation response were observed for one of the genes analyzed, DDB2. After investigation, it was determined that these differences were due to primer design, since the primers used for qPCR were not covering all the variants detected by sequencing, demonstrating the power of this technology for exploring the multiplicity of transcripts expressed. It has been previously reported that ionizing radiation has a regulatory influence on alternative transcription of specific radiation-responsive genes (*54, 55*). Therefore, since modulation of gene variants is expected after radiation exposure in blood samples, nanopore sequencing analysis is a unique tool to obtain a complete expression profile picture of radiation-responsive genes, by identifying all responsive variants expressed as long as its expression level is compatible with the number of reads analyzed (i.e., frequency of expression compatible with the number of reads, superior to 1, in 40–75 million reads). qPCR analyses cannot allow this, since new primers must be redesigned to include all the radiation-responsive variants of the genes, and this can only be done for those identified and for which the sequence is known.

KEGG analysis of the DEGs identified p53 signaling pathway as the most enriched pathway. This is not surprising, since P53 is the master regulator of the cellular radiation response and many of the genes identified are p53 dependent (*56*). The cytokine-cytokine receptor interaction pathway was also enriched, suggesting a radiation-induced inflammatory response as has been previously observed *ex vivo* (*57*) and *in vivo* in humans (*58*). Not surprisingly, apoptosis was also highly represented by the DEGS, as the programmed cell death, the most important cell death pathway after radiation exposure, is mainly regulated by radiation-induced double-strand breaks (*59*).

With the risk of an acute large-scale radiological/nuclear incident of a large population, and the limited capacity of existing techniques, there is clearly a need for developing and establishing new, rapid and high-throughput biodosimetric tools for estimation of received dose and initial triage. Classic biodosimetry assays, such as dicentric or micronucleus, can provide accurate dose estimates. However, they are time-consuming and low-throughput methodologies (*1, 60, 61*), difficult to apply in an emergency situation where large sample screenings in a short period of time are required (within 24 h). In this study we demonstrated the usefulness of nanopore sequencing to precisely identify radiation-responsive transcripts, making this a technology of great interest for biological dosimetry. We analyzed the number of read counts and found clear differences in the number of gene transcripts between control and irradiated samples (Fig. 3A). Under the hypothesis of the necessity to analyze an unknown sample without a control (''real life'' situation), it would therefore be possible, using this technology, to differentiate exposed and non-exposed individuals by establishing a threshold for the irradiated profile, based on the frequency of reads of a particular transcript in a defined time window of sequencing (Fig. 8). For instance, considering APOBEC3H counts, we calculated that, by analyzing the first 50,000 reads, which could be achieved in approximately <3 min, 0.96 counts will be obtained in non-exposed blood samples while 17 counts would be obtained in 2 Gy irradiated blood samples. These assumptions are extrapolated from the data obtained from 50 million reads performed in this study (Fig. 3). This difference in number of counts could help identify exposed individuals for triage purposes. Since nanopore sequencing can be analyzed in real-time, establishing the counts per sequencing time of specific biomarkers in response to radiation would offer a rapid and high-throughput method to identify the unexposed, and those exposed to high-dose radiation (>2 Gy) (Fig. 8). Individuals exposed to high doses may develop acute radiation syndrome, especially the hematological syndrome requiring hospitalization and specific treatment (*24*). This theoretical time will be tested and demonstrated in future studies to address the effect of inter-individual variability in response to radiation. We have participated in several exercises in the past years (*16, 18, 19*) where we provided robust dose estimates from blood samples where a donor-match control was not available. In these cases we compared the level of expression in these unknown samples with an existing calibration curve produced in our laboratory, pooling blood RNAs from 10 donors of mixed age and gender, and obtained satisfying results. It should also be noted that the data generated in this study were already obtained using several donors (9) and therefore already partially reflect inter-individual variability. Future studies will be undertaken to more accurately determine the count ranges necessary for distinguishing a control sample from an

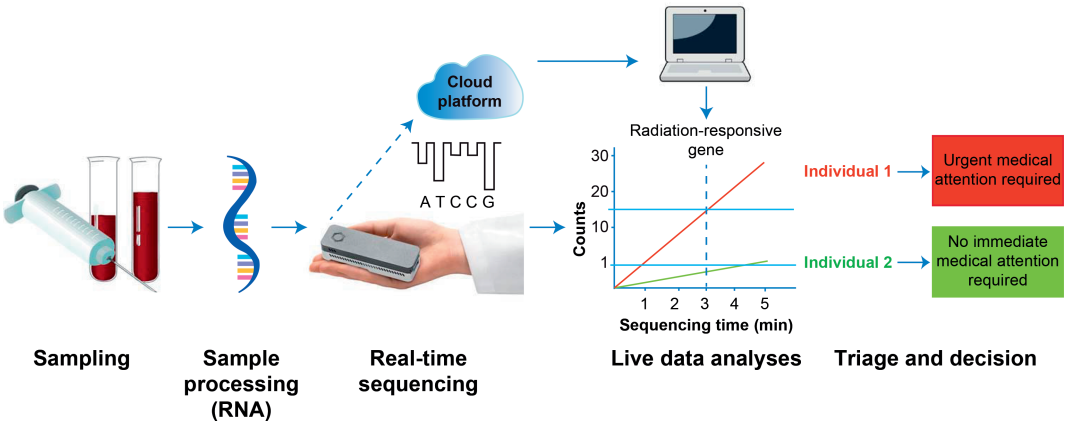

FIG. 8. Biodosimetry workflow. Future research will continue in the direction of the development of a fast-analytical platform by using portable third-generation sequencing technology and the panel of genes presented in this study.

irradiated one. In addition, although dedicated bioinformatic tools must be developed, the pocket-size devices currently available would permit sequencing analysis to be performed in real-time, in the field, without the need for shipping blood samples to specialized laboratories (Fig. 8). Also, this platform, with the specific gene panel, could provide a medical diagnostic tool to determine patient-specific radiation sensitivity for predicting normal tissue responses to radiation, ultimately personalizing treatments to prevent normal tissue radiotoxicity.

Biological dosimetry applications of nanopore sequencing are still under development in our laboratory and specific steps in the protocol require further modification for use of this technology as a rapid screening platform for blood-based detection of radiation exposure. For instance, sample preparation time required for the sequencing analysis will require shortening since the RNA extraction and library preparation is performed in 90 and 165 min, respectively. Moreover, the RNA requirements used in the current study necessitate blood volumes higher than what would ideally be requested. It should be noted that Oxford Nanopore Technologies has already improved this issue in their available kits for sequencing. We have used 1 ng of poly(A)+-enriched RNA, but the current methodology can now be performed by analyzing only 50 ng of total RNA, thereby reducing the sample preparation time and the blood volume required to approximately 1–2 ml for such analysis. Additionally, instead of sequencing the whole transcriptome, as was done in the current study, targeted sequencing could be performed using gene-specific primers; the library preparation time would be the same, but it would provide far higher sequencing depth for transcripts of interest or low expressed transcript variants and would highly simplify the bioinformatic analysis.

In summary, although optimization is required, to our knowledge this is the first study in which nanopore sequencing is used in human blood, providing radiation-induced transcriptomic signatures, new biomarkers of radiation exposure, and establishing the basis for the development of a biodosiemtry sequencing platform. The findings from this work will help guide future research, and suggest that the technology can be used to develop a quick and high-throughput platform for assessing radiation exposure.

SUPPLEMENTARY INFORMATION

Table S1. Information about age and gender from the healthy donors involved in the dose-response and sequencing analysis experiments.

Table S2. Primer sequences used for qPCR analysis.

Table S3. Differentially-expressed genes identified by nanopore sequencing in response to radiation in order of significance (by *P* value).

Table S4. qPCR analysis performed in the sequenced samples (Fig. 3B).

Fig. S1. Linear regression analysis of the correlation between qPCR and sequencing analyses.

Fig. S2. Dose-response curves adjusted by linear regression model for APOBEC3H and FDXR.

Fig. S3. Dose-response curves adjusted by linear regression model for APOBEC3H.

Fig. S4. Dose-response curves adjusted by linear regression model for FDXR.

ACKNOWLEDGMENTS

Financial support for this work was provided by the Radiation Theme of the Newcastle University and PHE Health Protection Research Unit (HPRU). Additional support was provided to MIL by the National Institutes of Health (NIH grant nos. R01 HG009937, R01 MH118349, P01 CA142538 and P30 ES010126).

Received: July 18, 2019; accepted: November 12, 2019; published online: December 12, 2019

REFERENCES

1. Hall J, Jeggo PA, West C, Gomolka M, Quintens R, Badie C, et al. Ionizing radiation biomarkers in epidemiological studies – An update. Mutat Res 2017; 771:59–84.

2. Tichy A, Kabacik S, O'Brien G, Pejchal J4 Sinkorova Z, Kmochova A, et al. The first in vivo multiparametric comparison of different radiation exposure biomarkers in human blood. PLOS One 2018; 13:e0193412.
3. Ainsbury E, Badie C, Barnard S, Manning G, Moquet J, Abend M, et al. Integration of new biological and physical retrospective dosimetry methods into EU emergency response plans - joint RENEB and EURADOS inter-laboratory comparisons. Int J Radiat Biol 2017; 93:99–109.
4. Kulka U, Abend M, Ainsbury E, Badie C, Barquinero JF, Barrios L, et al. RENEB - Running the European Network of biological dosimetry and physical retrospective dosimetry. Int J Radiat Biol 2017; 93:2–14.
5. Meadows SK, Dressman HK, Muramoto GG, Himburg H, Salter A, Wei ZZ, et al. Gene expression signatures of radiation response are specific, durable and accurate in mice and humans. PLoS One 2008; 3.
6. Knops K, Boldt S, Wolkenhauer O, Kriehuber R. Gene expression in low- and high-dose-irradiated human peripheral blood lymphocytes: Possible applications for biodosimetry. Radiat Res 2012; 178:304–12.
7. Kabacik S, Manning G, Raffy C, Bouffler S, Badie C. Time, dose and ataxia telangiectasia mutated (ATM) status dependency of coding and noncoding rna expression after ionizing radiation exposure. Radiat Res 2015; 183:325–37.
8. Manning G, Kabacik S, Finnon P, Bouffler S, Badie C. High and low dose responses of transcriptional biomarkers in ex vivo X-irradiated human blood. Int J Radiat Biol 2013; 89:512–22.
9. Kabacik S, Ortega-Molina A, Efeyan A, Finnon P, Bouffler S, Serrano M, et al. A minimally invasive assay for individual assessment of the ATM/CHEK2/p53 pathway activity. Cell Cycle 2011; 10:1152–61.
10. Kabacik S, Mackay A, Tamber N, Manning G, Finnon P, Paillier F, et al. Gene expression following ionising radiation: identification of biomarkers for dose estimation and prediction of individual response. Int J Radiat Biol 2011; 87:115–29.
11. Ghandhi SA, Smilenov LB, Elliston CD, Chowdhury M, Amundson SA. Radiation dose-rate effects on gene expression for human biodosimetry. BMC Med Genomics 2015; 8:22.
12. Paul S, Barker CA, Turner HC, McLane A, Wolden SL, Amundson SA. Prediction of in vivo radiation dose status in radiotherapy patients using ex vivo and in vivo gene expression signatures. Radiat Res 2011; 175:257–65.
13. Cruz-Garcia L, O'Brien G, Donovan E, Gothard L, Boyle S, Laval A, et al. Influence of confounding factors on radiation dose estimation using in vivo validated transcriptional biomarkers. Health Phys 2018; 115:90–101.
14. O'Brien G, Cruz-Garcia L, Majewski M, Grepl J, Abend M, Port M, et al. FDXR is a biomarker of radiation exposure in vivo. Sci Rep 2018; 8:684.
15. Brzoska K, Kruszewski M. Toward the development of transcriptional biodosimetry for the identification of irradiated individuals and assessment of absorbed radiation dose. Radiat Environ Biophys 2015; 54:353–63.
16. Abend M, Badie C, Quintens R, Kriehuber, G. Manning, E. Macaeva, et al. Examining radiation-induced in vivo and in vitro gene expression changes of the peripheral blood in different laboratories for biodosimetry purposes: First RENEB Gene Expression Study. Radiat Res 2016; 185:109–23.
17. Polozov S, Cruz-Garcia L, Badie C. Rapid gene expression based dose estimation for radiological emergencies. Radiat Prot Dosim 2019.
18. Badie C, Kabacik S, Balagurunathan Y, Bernard N, Brengues M, Faggioni G, et al. Laboratory intercomparison of gene expression assays. Radiat Res 2013; 180:138–48.
19. Manning G, Macaeva E, Majewski M, Kriehuber R, Brzoska K, Abend M, et al. Comparable dose estimates of blinded whole blood samples are obtained independently of culture conditions and analytical approaches. Second RENEB gene expression study. Int J Radiat Biol 2017; 93:87–98.
20. Lee Y, Pujol Canadell M, Shuryak I, Jay R. Perrier, Maria Taveras, Purvi Patel, et al. Candidate protein markers for radiation biodosimetry in the hematopoietically humanized mouse model. Sci Rep 2018; 8:13557–57.
21. Meadows SK, Dressman HK, Daher P, Himburg H, Russell JL, Doan P, et al. Diagnosis of partial body radiation exposure in mice using peripheral blood gene expression profiles. PLOS One 2010; 5:e11535.
22. Mukherjee S, Laiakis EC, Fornace AJ, Amundson SA. Impact of inflammatory signaling on radiation biodosimetry: mouse model of inflammatory bowel disease. BMC Genomics 2019; 20:329.
23. Paul S, Amundson SA. Development of gene expression signatures for practical radiation biodosimetry. Int J Radiat Oncol Biol Phys 2008; 71:1236–44.
24. Port M, Ostheim P, Majewski M, Voss T, Haupt J, Lamkowski A, et al. Rapid high-throughput diagnostic triage after a mass radiation exposure event using early gene expression changes. Radiat Res 2019; 192:208–18.
25. Chaudhry MA, Omaruddin RA, Brumbaugh CD, Tariq MA, Pourmand N. Identification of radiation-induced microRNA transcriptome by next-generation massively parallel sequencing. J Radiat Res 2013; 54:808–22.
26. Jaksik R, Iwanaszko M, Rzeszowska-Wolny J, Kimmel M. Microarray experiments and factors which affect their reliability. Biol Direct 2015;10:46–46.
27. Zhang J, Chiodini R, Badr A, Zhang G. The impact of next-generation sequencing on genomics. J Genet Genomics 2011; 38:95–109.
28. Rhoads A, Au KF. PacBio sequencing and its applications. Genomics Proteomics Bioinformatics 2015; 13:278–89.
29. Lu H, Giordano F, Ning Z. Oxford Nanopore MinION Sequencing and Genome Assembly. Genomics Proteomics Bioinformatics 2016; 14:265–79.
30. Clarke J, Wu H-C, Jayasinghe L, Patel A, Reid S, Bayley H. Continuous base identification for single-molecule nanopore DNA sequencing. Nat Nanotechnol 2009; 4:265–70.
31. Jain M, Koren S, Miga KH, Quick J, Rand AC, Sasani TA, et al. Nanopore sequencing and assembly of a human genome with ultra-long reads. Nat Biotechnol 2018; 36:338.
32. Ardui S, Ameur A, Vermeesch JR, Hestand MS. Single molecule real-time (SMRT) sequencing comes of age: applications and utilities for medical diagnostics. Nucleic Acids Res 2018; 46:2159–68.
33. Pomerantz A, Penafiel N, Arteaga A, Bustamante L, Pichardo F, Coloma LA, et al. Real-time DNA barcoding in a rainforest using nanopore sequencing: opportunities for rapid biodiversity assessments and local capacity building. Gigascience 2018; 7:giy033.
34. Edwards A, Debbonaire AR, Sattler B, Mur LAJ, Hodson AJ. Extreme metagenomics using nanopore DNA sequencing: a field report from Svalbard, 78°N. bioRxiv 2016; 073965.
35. Castro-Wallace SL, Chiu CY, John KK, Stahl SE, Rubins KH, McIntyre ABR, et al. Nanopore DNA sequencing and genome assembly on the International Space Station. Sci Rep 2017; 7:18022.
36. Moquet J, Higueras M, Donovan E, Boyle S, Barnard S, Bricknell C, et al. Dicentric dose estimates for patients undergoing radiotherapy in the RTGene Study to assess blood dosimetric models and the new Bayesian method for gradient exposure. Radiat Res 2018; 190:596–604.
37. Love MI, Soneson C, Patro R. Swimming downstream: statistical analysis of differential transcript usage following salmon quantification. Version 3. F1000Res 2018; 7:952.
38. Li H. Minimap2: pairwise alignment for nucleotide sequences. Bioinformatics 2018; 34:3094–100.
39. Patro R, Duggal G, Love MI, Irizarry RA, Kingsford C. Salmon

provides fast and bias-aware quantification of transcript expression. Nat Methods 2017; 14:417.

40. McCarthy DJ, Chen Y, Smyth GK. Differential expression analysis of multifactor RNA-Seq experiments with respect to biological variation. Nucleic Acids Res 2012; 40:4288–97.

41. Paul S, Amundson SA. Gene expression signatures of radiation exposure in peripheral white blood cells of smokers and nonsmokers. Int J Radiat Biol 2011; 87:791–801.

42. Harris RS, Dudley JP. APOBECs and virus restriction. Virology 2015; 479–480:131–45.

43. Stelzer G, Rosen N, Plaschkes I, Zimmerman S, Twik M, Fishilevich S, et al. The GeneCards Suite: From gene data mining to disease genome sequence analyses. Curr Protoc Bioinformatics 2016; 54:1.30.1–33.

44. Kang C-M, Park K-P, Song J-E, Jeoung D, Cho C-K, Kim TH, et al. Possible biomarkers for ionizing radiation exposure in human peripheral blood lymphocytes. Radiat Res 2003; 159:312–19.

45. Ghandhi SA, Shuryak I, Morton SR, Amundson SA, Brenner DJ. New approaches for quantitative reconstruction of radiation dose in human blood cells. bioRxiv 2019; 640052.

46. Lee K-F, Weng JT-Y, Hsu PW-C, Chi YH, Chen CK, Liu IY, et al. Gene expression profiling of biological pathway alterations by radiation exposure. J Biomed Res Int 2014; 2014:834087.

47. Pei B, Sisu C, Frankish A, Howald C, Habegger L, Jasmine X, et al. The GENCODE pseudogene resource. Genome Biol 2012; 13:R51.

48. Hawkins PG, Morris KV. Transcriptional regulation of Oct4 by a long non-coding RNA antisense to Oct4-pseudogene 5. Transcription 2010; 1:165–75.

49. Tam OH, Aravin AA, Stein P, Girard A, Murchison EP, Cheloufi S, et al. Pseudogene-derived small interfering RNAs regulate gene expression in mouse oocytes. Nature 2008; 453:534–38.

50. Liu F, Xing L, Zhang X, Zhang X. A four-pseudogene classifier identified by machine learning serves as a novel prognostic marker for survival of osteosarcoma. Genes (Basel) 2019; 10:414.

51. Song H, Yang J, Zhang Y, Zhou J, Li Y, Hao X. Integrated analysis of pseudogene RP11-564D11.3 expression and its potential roles in hepatocellular carcinoma. Epigenomics 2019; 11:267–80.

52. Rouchka EC, Flight RM, Fasciotto BH, Estrada R, Eaton JW, Patibandla PK, et al. Elucidation of dose-dependent transcriptional events immediately following ionizing radiation exposure. bioRxiv 2017; 207951.

53. Nongrum S, Vaiphei ST, Keppen J, Ksoo M, Kashyap E, Sharan RN. Identification and preliminary validation of radiation response protein(s) in human blood for a high-throughput molecular biodosimetry technology for the future. Genome Integr 2017; 8:5.

54. Macaeva E, Saeys Y, Tabury K, Janssen A, Michaux A, Benotmane MA, et al. Radiation-induced alternative transcription and splicing events and their applicability to practical biodosimetry. Sci Rep 2016; 6:19251.

55. Forrester HB, Li J, Hovan D, Ivashkevich AN, Sprung CN. DNA repair genes: Alternative transcription and gene expression at the exon level in response to the DNA damaging agent, ionizing radiation. PLOS One 2012; 7:e53358.

56. Riley T, Sontag E, Chen P, Levine A. Transcriptional control of human p53-regulated genes. Nat Rev Mol Cell Biol 2008; 9:402–12.

57. El-Saghire H, Thierens H, Monsieurs P, Mihaux A, Vandevoorde C, Baatout S. Gene set enrichment analysis highlights different gene expression profiles in whole blood samples X-irradiated with low and high doses. Int J Radiat Biol 2013; 89:628–38.

58. Manning G, Tichy A, Sirak I, Badie C. Radiotherapy-associated long-term modification of expression of the inflammatory biomarker genes ARG1, BCL2L1, and MYC. Front Immunol 2017; 8:412.

59. Liu B, Bhatt D, Oltvai ZN, Greenberger JS, Bahar I. Significance of p53 dynamics in regulating apoptosis in response to ionizing radiation, and polypharmacological strategies. Sci Rep 2014; 4:6245.

60. Pernot E, Hall J, Baatout S, Benotmane MA, Blanchardon E, Bouffler S, et al. Ionizing radiation biomarkers for potential use in epidemiological studies. Mutat Res 2012; 751:258–86.

61. Rothkamm K, Beinke C, Romm H, Badie C, Balagurunathan Y, Barnard S, et al. Comparison of established and emerging biodosimetry assays. Radiat Res 2013; 180:111–9.